Nonlinear MHD Effects on the Alfvén Eigenmode Evolution

Y. Todo 1), H. L. Berk 2), B. N. Breizman 2)
1) National Institute for Fusion Science, Toki, Japan
2) Institute for Fusion Studies, University of Texas at Austin, Austin, United States

e-mail contact of main author: todo@nifs.ac.jp

Abstract. Two types of hybrid simulations of MHD fluid and energetic particles were carried out to investigate MHD nonlinear effects on Alfvén eigenmode evolution. The first type contains fully nonlinear effects of both the MHD fluid and the energetic particles. The second type of the simulation is similar to the first type but different in that the MHD equations are linearized. Comparison between the results of the two types of simulations clarifies the MHD nonlinear effects. A tokamak plasma, where a toroidal Alfvén eigenmode (TAE) with toroidal mode number n=4 is the most unstable, was investigated. When the saturation level is $\delta B/B \sim 2\times10^{-2}$ in the linear MHD simulation results, we found that the saturation level is $\delta B/B \sim 8\times10^{-3}$ in the nonlinear MHD simulation results. The MHD nonlinear effects suppress the saturation level of the TAE. Detailed analyses indicate that the suppression effect arises from the change in n=0 harmonics of the magnetic field that is generated by the nonlinear electric field $-\mathbf{v}_{TAE}\times\delta\mathbf{B}_{TAE}$, a product of the velocity field and the magnetic field of the TAE. Axisymmetric velocity fields are also generated in the nonlinear run, although the change in the n=0 magnetic field plays the dominant role in the suppression of TAE.

1. Introduction

For time evolution of Alfvén eigenmodes, an important nonlinearity arises from the dynamics of energetic particles that destabilize the Alfvén eigenmodes. It was demonstrated by computer simulations that the particle trapping cause the saturation of toroidal Alfvén eigenmodes (TAE) [1-4]. This enables reduced simulations of TAE, where spatial profiles and damping rates of TAEs are assumed to be independent of mode amplitude. TAE bursts at a Tokamak Fusion Test Reactor experiment were reproduced by a reduced simulation [5]. Many aspects of the TAE bursts were well reproduced, while only the saturation amplitude was $\delta B/B \sim 2\times10^{-2}$ which is higher than the value $\delta B/B \sim 10^{-3}$ inferred from the experimental plasma displacement [5,6]. In another simulation run of TAE bursts, where the MHD nonlinear effects are taken account, the saturation level is lower than $\delta B/B \sim 10^{-2}$ [7]. These simulation results motivate us to investigate the MHD nonlinear effects.

Two types of hybrid simulations of MHD fluid and energetic particles were carried out to investigate MHD nonlinear effects on Alfvén eigenmode evolution using MEGA code [8,9] and a linearized version of MEGA code. Fully nonlinear effects of both the MHD fluid and the energetic particles are contained in MEGA code. In the linearized version of MEGA code, the MHD equations are linearized while the nonlinear particle dynamics are followed. In this paper, simulation results of the two types of simulations are presented and compared. It is demonstrated that the MHD nonlinear effects suppress the saturation level of the TAE. Detailed analyses indicate that the suppression effect arises from the change in n=0 harmonics of the magnetic field that is generated by the nonlinear electric field $-\mathbf{v}_{TAE}\times\delta\mathbf{B}_{TAE}$, a product of the velocity field and the magnetic field of the TAE.

2. Simulation Model

The hybrid simulation model for MHD and energetic particles [2,8-10] is employed in MEGA code. Plasma is divided into bulk plasma and energetic ions. The bulk plasma is described by the nonlinear full MHD equations. The electromagnetic field is given by the MHD description.

This approximation is reasonable under the condition that the energetic ion density is much less than the bulk plasma density. The MHD equations with energetic ion effects are,

$$\frac{\partial \rho}{\partial t} = -\nabla \cdot (\rho \mathbf{v}) \tag{1}$$

$$\rho \frac{\partial}{\partial t}\mathbf{v} = -\rho\vec{\omega}\times\mathbf{v} - \rho\nabla\left(\frac{v^2}{2}\right) - \nabla p + (\mathbf{j} - \mathbf{j}'_h)\times\mathbf{B} + \nu\rho\left[\frac{4}{3}\nabla(\nabla\cdot\mathbf{v}) - \nabla\times\vec{\omega}\right] \tag{2}$$

$$\frac{\partial \mathbf{B}}{\partial t} = -\nabla \times \mathbf{E} \tag{3}$$

$$\frac{\partial p}{\partial t} = -\nabla\cdot(p\mathbf{v}) - (\gamma-1)p\nabla\cdot\mathbf{v} + (\gamma-1)\left[\nu\rho\omega^2 + \frac{4}{3}\nu\rho(\nabla\cdot\mathbf{v})^2 + \eta\mathbf{j}\cdot(\mathbf{j}-\mathbf{j}_{eq})\right] \tag{4}$$

$$\mathbf{E} = -\mathbf{v}\times\mathbf{B} + \eta(\mathbf{j} - \mathbf{j}_{eq}) \tag{5}$$

$$\mathbf{j} = \frac{1}{\mu_0}\nabla\times\mathbf{B} \tag{6}$$

$$\vec{\omega} = \nabla\times\mathbf{v} \tag{7}$$

where μ_0 is the vacuum magnetic permeability, γ is the adiabatic constant, ν is an artificial viscosity coefficient chosen to maintain numerical stability and all the other quantities are conventional. Here, $\mathbf{j}_h'$ is the energetic ion current density without $\mathbf{E}\times\mathbf{B}$ drift. The effect of the energetic ions on the MHD fluid is taken into account in the MHD momentum equation [Eq. (2)] through the energetic ion current. The MHD equations are solved using a finite difference scheme of fourth order accuracy in space and time.

In the linear MHD simulation, the following equations are solved:

$$\frac{\partial \rho}{\partial t} = -\nabla \cdot (\rho_{eq} \mathbf{v}) \tag{8}$$

$$\rho_{eq} \frac{\partial}{\partial t}\mathbf{v} = -\nabla p_{eq} + (\mathbf{j}_{eq} - \mathbf{j}'_{h\,eq})\times\delta\mathbf{B} + (\delta\mathbf{j} - \delta\mathbf{j}'_h)\times\mathbf{B}_{eq} + \nu\rho\left[\frac{4}{3}\nabla(\nabla\cdot\mathbf{v}) - \nabla\times\vec{\omega}\right] \tag{9}$$

$$\frac{\partial \mathbf{B}}{\partial t} = -\nabla \times \mathbf{E} \tag{10}$$

$$\frac{\partial p}{\partial t} = -\nabla\cdot(p_{eq}\mathbf{v}) - (\gamma-1)p_{eq}\nabla\cdot\mathbf{v} \tag{11}$$

$$\mathbf{E} = -\mathbf{v}\times\mathbf{B}_{eq} + \eta(\mathbf{j} - \mathbf{j}_{eq}) \tag{12}$$

$$\mathbf{j} = \frac{1}{\mu_0}\nabla\times\mathbf{B} \tag{13}$$

$$\vec{\omega} = \nabla\times\mathbf{v} \tag{14}$$

The drift-kinetic description is employed for the energetic ions. The energetic ion current density without $\mathbf{E}\times\mathbf{B}$ drift in Eq. (2) includes the contributions from parallel velocity, curvature and gradient drifts, and magnetization current. The $\mathbf{E}\times\mathbf{B}$ drift disappears in $\mathbf{j}'_h$ due to quasi-neutrality [8].

It is important to start the simulations from MHD equilibria consistent with energetic ion distributions. When the energetic ion pressure is isotropic in the velocity space, the energetic ion contribution in Eq. (2) is just a scalar pressure gradient in the same form as the bulk pressure gradient [8]. Then, the equilibrium can be obtained from the Grad-Shafranov equation neglecting the energetic ion orbit width. However, if the energetic ion pressure is anisotropic in the velocity space and/or the energetic ion orbit width is not negligibly small, the Grad-Shafranov equation should be extended. We solve an extended Grad-Shafranov equation developed in Ref. [11] in the cylindrical coordinates (R, φ, z) where R is the major radius coordinate, φ is the toroidal angle coordinate, and z is the vertical coordinate. Details of the kinetic equilibrium construction is reported in Ref. 9.

3. Simulation Results

A tokamak plasma with aspect ratio of 3.2 was investigated. The spatial profiles of safety factor and beam ion beta are shown in Fig.1. The maximum velocity of beam ions is $1.2 v_A$. Here, v_A denotes Alfvén velocity at the plasma center. The ratio of the beam ion parallel Larmor radius to the minor radius is 0.09 for beam ion velocity equal to the Alfvén velocity. The magnetic moment is assumed to be zero to for simplicity. The number of grid points are $101 \times 100 \times 101$ for the cylindrical coordinates (R, φ, z). The viscosity and resistivity are chosen $\nu = 10^{-6} v_A R_0$ and $\eta = 10^{-6} \mu_0 v_A R_0$, respectively.

For the equilibrium condition mentioned above, we found that the toroidal Alfvén eigenmodes (TAE) with toroidal mode numbers n=3-5 are linearly unstable. The spatial profile of the most unstable TAE with n=4 is shown in Fig. 2. The frequency of the TAE with n=4 is located inside the gap of the Alfvén continuous spectra, as shown in Fig. 3.

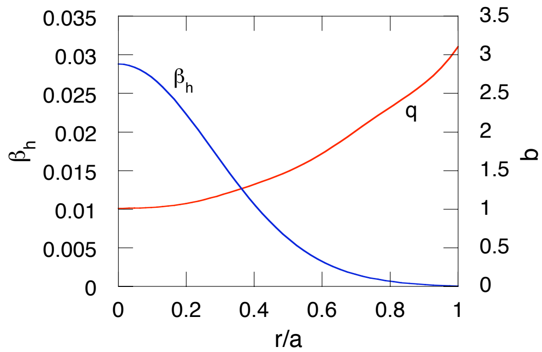

Fig.1 Spatial profiles of beam ion beta and safety factor.

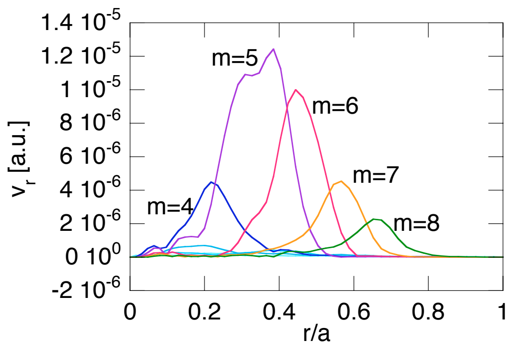

Fig.2 Spatial profile of each poloidal harmonic of the toroidal Alfvén eigenmode with toroidal mode number n=4.

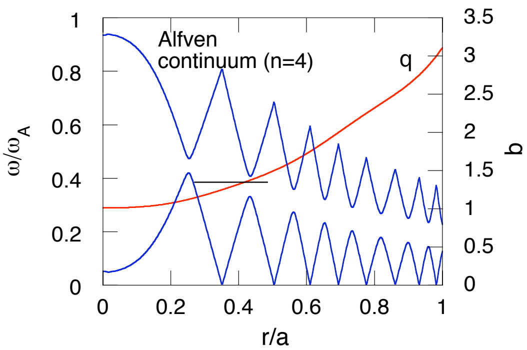

Fig.3 Frequency and location of the toroidal Alfvén eigenmode with toroidal mode number n=4. Alfvén continuous spectra are represented by blue curves. The safety factor profile is represented by red curve.

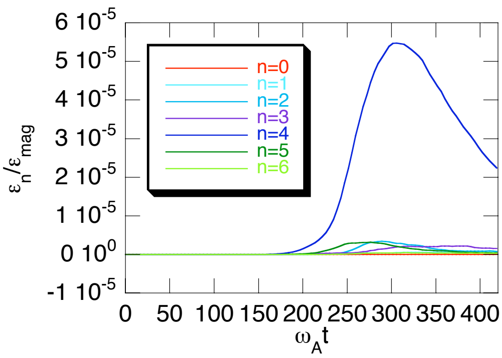

Fig.4 Time evolution of energy for each toroidal mode number in the linear MHD run.

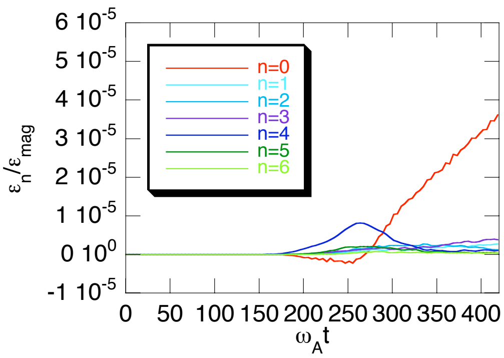

Fig.5 Time evolution of energy for each toroidal mode number in the standard nonlinear MHD run.

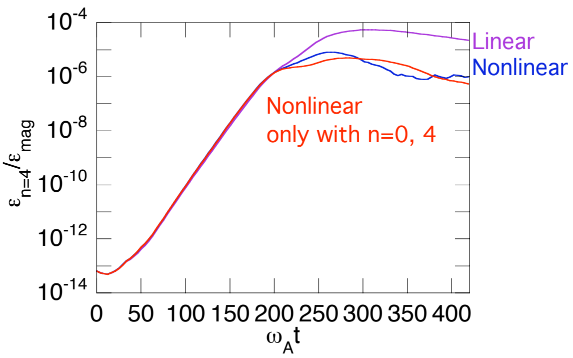

Fig.6 Comparison of energy evolution of toroidal mode number n=4 between the standard nonlinear MHD run (blue curve), the linear MHD run (violet curve), and the nonlinear MHD run where only n=0, 4 modes are retained (red curve).

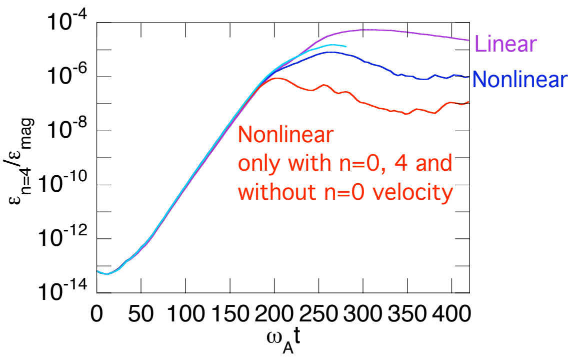

Fig.7 Comparison of energy evolution of toroidal mode number n=4 between the standard nonlinear MHD run (blue curve), the linear MHD run (violet curve), and the nonlinear MHD run where only n=0, 4 modes are retained and the n=0 velocity field is removed (red curve). Light blue curve represents a run where only n=0, 4 modes are retained and the n=0 magnetic field is removed.

A linear MHD simulation and a nonlinear MHD simulation were carried out. The evolution of energy for each toroidal mode number is shown in Fig. 4 for the linear run and in Fig. 5 for the nonlinear run. The n=4 TAE is the most unstable and is saturated at $\omega_A t = 300$ in Fig. 4 and at $\omega_A t = 260$ in Fig. 5. Comparing Figs. 4 and 5, the saturation level of the n=4 mode energy in the nonlinear MHD run is 15% of that in the linear MHD run. The saturation amplitude of the n=4 TAE is $\delta B / B \sim 2 \times 10^{-2}$ in the linear MHD run, and $\delta B / B \sim 8 \times 10^{-3}$ in the nonlinear MHD run. MHD nonlinear effects suppress the TAE saturation level. We see in Fig. 5 that the n=0 mode energy continuously grows until the end of the simulation after the saturation of the n=4 mode energy. This suggests that the beam ions continue to drive TAEs while some nonlinear mechanism stabilizes them converting the TAE energy into the n=0 mode energy.

We carried out another nonlinear MHD run where toroidal mode numbers only n=0 and 4 are retained. The time evolution of energy for toroidal mode number n=4 is shown in Fig. 6 with those of the standard nonlinear run shown in Fig. 5 and the linear run shown in Fig. 4. The saturation level in the run with the selected modes is similar to the standard nonlinear run. This indicates that the TAE saturation level is suppressed by the n=0 harmonics rather than the harmonics with higher toroidal mode numbers. We carried out other two runs where only n=0 and 4 harmonics are retained and the n=0 velocity field or the n=0 magnetic field is removed. The results are compared in Fig. 7. We see that the saturation level is the lowest when the n=0 velocity field is removed. These results indicate that the suppression effect arises from the change in n=0 harmonics of the magnetic field ($\delta\mathbf{B}_{n=0}$). Since there is no n=0 velocity field in this run, $\delta\mathbf{B}_{n=0}$ is generated by a nonlinear electric field $\mathbf{E}_{n=0} = -\mathbf{v}_{n=4} \times \delta\mathbf{B}_{n=4}$, which is the nonlinear electric field of the TAE. The lowest saturation level without the n=0 velocity field implies that the n=0 velocity field relaxes $\delta\mathbf{B}_{n=0}$ and its suppression effect.

It is not clear why $\delta\mathbf{B}_{n=0}$ suppresses the TAE saturation level. We show in Fig. 8 the Alfvén continuous spectra and the safety factor profile at $\omega_A t = 280$ in the standard nonlinear MHD run. In Fig. 5 the growth of the n=4 mode energy is saturated just before this time. We see that the safety factor profile is steepened near the n=4 TAE spatial peak at $r/a \sim 0.4$. The n=0 poloidal velocity field at the same time in the standard nonlinear MHD run is shown in Fig. 9. The poloidal harmonics m=0 and 1 are dominant in the n=0 poloidal velocity field. The poloidal velocity field sharply peaks near the n=4 TAE spatial peak.

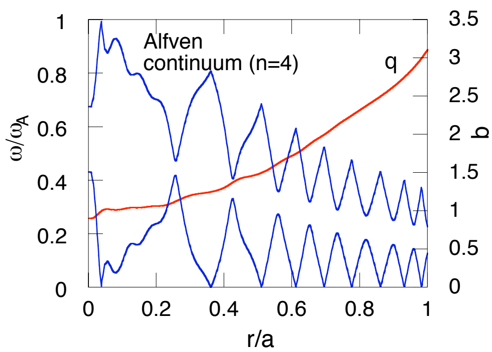

Fig.8 Alfvén continuous spectra with the toroidal mode number n=4 and the safety factor profile at $\omega_A t = 280$ in the standard nonlinear run.

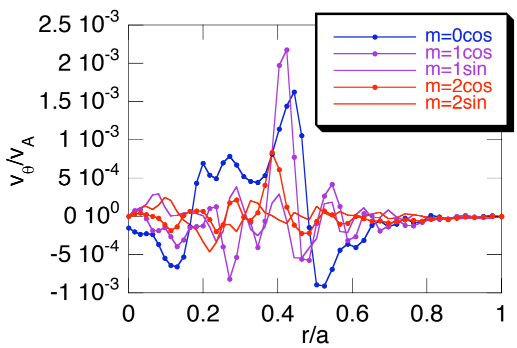

Fig.9 Poloidal velocity field with the toroidal mode number n=0 at $\omega_A t = 280$ in the standard nonlinear run.

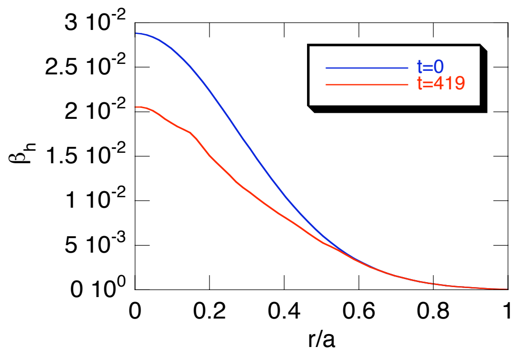

Fig.10 Initial and final beam ion beta profile in the linear MHD run.

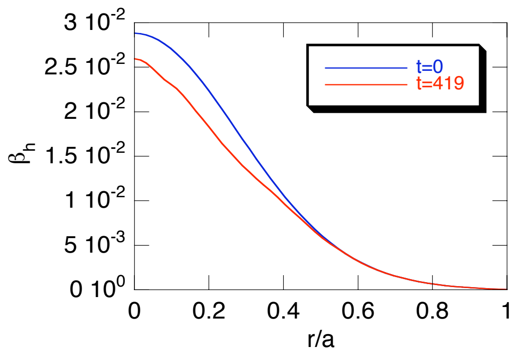

Fig.11 Initial and final beam ion beta profile in the standard nonlinear MHD run.

Initial and final beam ion beta profiles are compared in Fig. 10 for the linear MHD run and in Fig. 11 for the standard nonlinear MHD run. We see that the beam ion transport is also suppressed by the MHD nonlinear effects.

4. Discussion and Summary

Saturation of TAE instability due to MHD nonlinear effects was theoretically investigated in Ref. 12. Comparison between the present simulation results and the theory in Ref. 12 is needed. The change in safety factor profile and the generation of $\mathbf{E}\times\mathbf{B}$ flow were found in a computer simulation where energetic particles are approximated by the Landau Fluid model [13]. In Ref. 13, it is reported that the $\mathbf{E}\times\mathbf{B}$ flow has the dominant effects on the saturation of the TAE instability. On the other hand, in the present simulation results, it was found that the change in the n=0 magnetic field suppresses the saturation level of the TAE.

In this paper, the two types of simulation results were presented and compared. In the first type of the simulation the fully nonlinear MHD equations are solved, while linearized MHD equations are employed in the second type. A tokamak plasma, where a toroidal Alfvén eigenmode (TAE) with toroidal mode number n=4 is the most unstable, was investigated. Comparison between the results of the two types of simulations clarified the MHD nonlinear effects. We found that the saturation level is $\delta B/B \sim 8\times10^{-3}$ in the nonlinear MHD simulation results when the saturation level is $\delta B/B \sim 2\times10^{-2}$ in the linear MHD simulation results. The MHD nonlinear effects suppress the saturation level of the TAE. Detailed analyses indicate that the suppression effect arises from the change in n=0 harmonics of the magnetic field that is generated by the nonlinear electric field $-\mathbf{v}_{TAE}\times\delta\mathbf{B}_{TAE}$, a product of the velocity field and the magnetic field of the TAE. Axisymmetric velocity fields are also generated in the nonlinear run, although the change in the n=0 magnetic field plays the dominant role in the suppression of TAE.

We have demonstrated that the MHD nonlinear effects suppress the TAE saturation level. It was also demonstrated by a computer simulation that the synchronized bursts of multiple TAEs take place with the MHD nonlinearity [7]. Thus, we can expect a simulation which reproduces the TAE bursts with saturation amplitude closer to that inferred from the experimental plasma displacement. On the other hand, as has been shown in this paper, energetic ion transport is also suppressed by the MHD nonlinearity. These results indicate that we need to focus on the feedback of the MHD fluid for the saturation level as well as beam ion transport in phase space when we try to simulate the TAE bursts.

References

[1] G. Y. Fu and W. Park, Phys. Rev. Lett. **74**, 1594 (1995).
[2] Y. Todo, T. Sato, K. Watanabe, T. H. Watanabe, and R. Horiuchi, Phys. Plasmas **2**, 2711 (1995).
[3] Y. Wu, R. B. White, Y. Chen, and M. N. Rosenbluth, Phys. Plasmas **2**, 4555 (1995).
[4] S. Briguglio, F. Zonca, and G. Vlad, Phys. Plasmas **5**, 3287 (1998).
[5] Y. Todo, H. L. Berk, and B. N. Breizman, Phys. Plasmas **10**, 2888 (2003).
[6] R. D. Durst, R. J. Fonck, K. L. Wong, C. Z. Cheng, E. D. Fredrickson, and S. F. Paul, Phys. Fluids B **4**, 3707 (1992).
[7] Y. Todo, T.-H. Watanabe, Hyoung-Bin Park, and T. Sato, Nuclear Fusion **41**, 1153 (2001).
[8] Y. Todo and T. Sato, Phys. Plasmas **5**, 1321 (1998).
[9] Y. Todo, K. Shinohara, M. Takechi, and M. Ishikawa, Phys. Plasmas **12**, 012503 (2005).
[10] W. Park et al., Phys. Fluids B **4**, 2033 (1992).
[11] E. V. Belova, N. N. Gorelenkov, and C. Z. Cheng, Phys. Plasmas **10**, 3240 (2003).
[12] F. Zonca, F. Romanelli, G. Vlad, and C. Kar, Phys. Rev. Lett. **74**, 698 (1995).
[13] D. A. Spong, B. A. Carreras, and C. L. Hedrick, Phys. Plasmas **1**, 1503 (1994).